Experimental Animals
Exp. Anim. 71(3), 391–398, 2022

Original

The cerebral artery in cynomolgus monkeys (*Macaca fascicularis*)

Keiichi TSUJI[1)], Shinichiro NAKAMURA[2,3)], Tomohiro AOKI[4)] and Kazuhiko NOZAKI[1)]

[1)]*Department of Neurosurgery, Shiga University of Medical Science, Seta Tsukinowa-cho, Otsu, Shiga 520-2192, Japan*
[2)]*Laboratory of Laboratory Animal Science, Azabu University, 1-17-71 Fuchinobe, Chuo-ku, Sagamihara, Kanagawa 252-5201, Japan*
[3)]*Research Center for Animal Life Science, Shiga University of Medical Science, Seta Tsukinowa-cho, Otsu, Shiga 520-2192, Japan*
[4)]*Department of Molecular Pharmacology, Research Institute, National Cerebral and Cardiovascular Center, 6-1 Kishibe-Shimmachi, Suita, Osaka 564-8565, Japan*

Abstract: Cerebral artery structure has not been extensively studied in primates. The aim of this study was to examine the cerebrovascular anatomy of cynomolgus monkeys (*Macaca fascicularis*), which are one of the most commonly used primates in medical research on human diseases, such as cerebral infarction and subarachnoid hemorrhage. In this study, we investigated the anatomy and diameter of cerebral arteries from 48 cynomolgus monkey brain specimens. We found three anatomical differences in the vascular structure of this species compared to that in humans. First, the distal anterior cerebral artery is single. Second, the pattern in which both the anterior inferior cerebellar artery and posterior inferior cerebellar artery branch from the basilar artery is the most common. Third, the basilar artery has the largest diameter among the major arteries. We expect that this anatomical information will aid in furthering research on cerebrovascular disease using cynomolgus monkeys.
Key words: anterior cerebral artery, cerebrovascular anatomy, cynomolgus monkey, diameter of cerebral artery, inferior cerebellar artery

Introduction

The structure of the anterior cerebral artery (ACA) differs depending on the monkey type. Specifically, similar to humans, orangutans present with two distal anterior cerebral arteries bilaterally [1]. In chimpanzees and rhesus monkeys, the proximal part of the anterior cerebral arteries on both sides are reported to be merged at the distal part [1]; additionally, studies have reported that the distal ACA is singular after the proximal arteries on both sides merge in rhesus monkeys [2, 3]. The anterior inferior cerebellar artery (AICA) and posterior inferior cerebellar artery (PICA) are reported as common trunks in the baboon [4]. However, in monkeys, the cerebellar artery structure has not been examined in depth.

As one of the experimental animals closest to humans, the cynomolgus monkey (*Macaca fascicularis*) is used for studying various diseases, such as infectious and neurodegenerative diseases [5]. Although cynomolgus monkeys are also used in the study of cerebrovascular disorders, such as subarachnoid hemorrhage [6–9] and cerebral infarction [10, 11], detailed cerebral vascular anatomy of cynomolgus monkeys is unavailable. To facilitate cerebrovascular disease research using cynomolgus monkeys, we investigated the cerebral vascular structure and blood vessel diameter from 48 cynomolgus monkey specimens.

(Received 7 January 2022 / Accepted 25 March 2022 / Published online in J-STAGE 20 April 2022)
Corresponding author: K. Tsuji. email: tsujikei@belle.shiga-med.ac.jp
Supplementary Table: refer to J-STAGE: https://www.jstage.jst.go.jp/browse/expanim

Materials and Methods

Forty-eight adult female cynomolgus monkey brains were used for this study. Of the 48 monkey brains, 17 were imported from China, 13 from Indonesia, 9 from Vietnam, 3 from the Philippines, and 2 from Cambodia. The remaining four brains were from monkeys bred at the study facility. The average age of the monkeys was 9.7 years (range: 4.9–15.6 years), and the average weight was 3.3 kg (range: 2.0–5.6 kg). All monkeys in this experiment were used in non-neurological research. The brains were used only in biogenetic technology, obstetrics and gynecology, and ophthalmology studies, and not in brain and cerebrovascular studies.

Of the 48 monkeys, 42 were euthanized at the conclusion of the experiment, and six died of a non-neurological illness. After the experiments complete, the monkeys were sedated with ketamine (5 mg/kg) and xylazine (1 mg/kg) intramuscularly, and then given 1–2 ml of pentobarbital sodium (64.8 mg/ml) until their eyelash reflex disappeared. Then, the left ventricle was punctured, and as much blood as possible was removed. After mandibular breathing was confirmed, 7–8 ml of pentobarbital sodium (64.8 mg/ml) was given transvenously. Once euthanasia was confirmed, intracranial arteries were perfused with physiological saline from the left ventricle to wash out the blood clots and then they were perfused with 10% formalin. Next, craniotomy was performed; the brains were extracted and fixed with 10% formalin. After the second day, the intracranial arteries were stripped under a microscope. Images of the cerebral artery were taken using a microscope with a camera (SMZ-O®, Nikon Corp., Tokyo, Japan) for the analysis of branching patterns and measurement of cerebral artery diameter (Fig. 1).

Next, the diameters of cerebral arteries of 33 monkeys of known age and weight were measured using ImageJ [12]. Six monkeys that died of disease were excluded. The outer diameter was measured as described for measuring cerebral artery diameter [13–15] (Fig. 2). The internal carotid artery (ICA) was measured distal to the anterior choroidal artery (AchA). The ACA was measured at the middle of the horizontal part of the ACA (A1) and at the distal portion where the bilateral ACA merged (A2). The middle cerebral artery (MCA) was measured at the middle of the ICA and bifurcation of the MCA (M1). The posterior cerebral artery (PCA) was measured at the middle of the top of the basilar artery

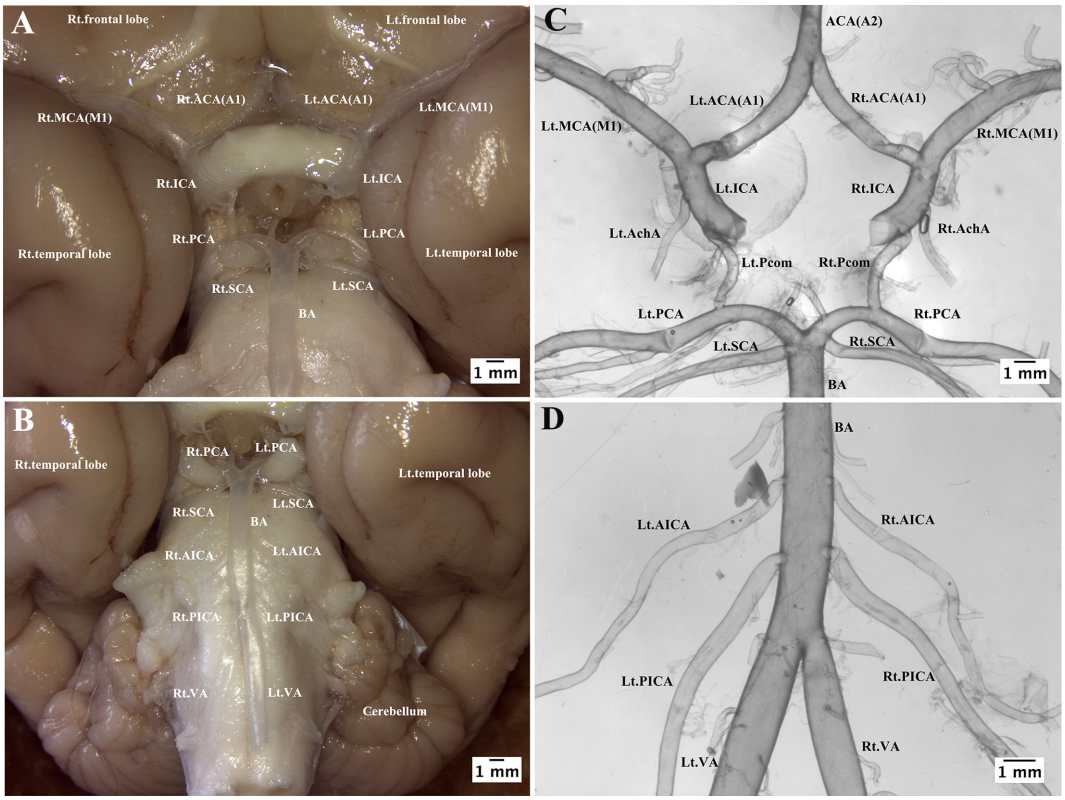

Fig. 1. The observation of cerebrum was conducted from the bottom of the frontotemporal lobes (A), and from the bottom of the cerebellar and brain stem (B). The Circle of Willis was observed after striping the intracranial arteries from the brain (C). The vertebral artery, basilar artery, and cerebellar arteries were also detected (D). In this figure, the anterior cerebral artery of the monkey is classified as single type.

 doi: 10.1538/expanim.22-0002

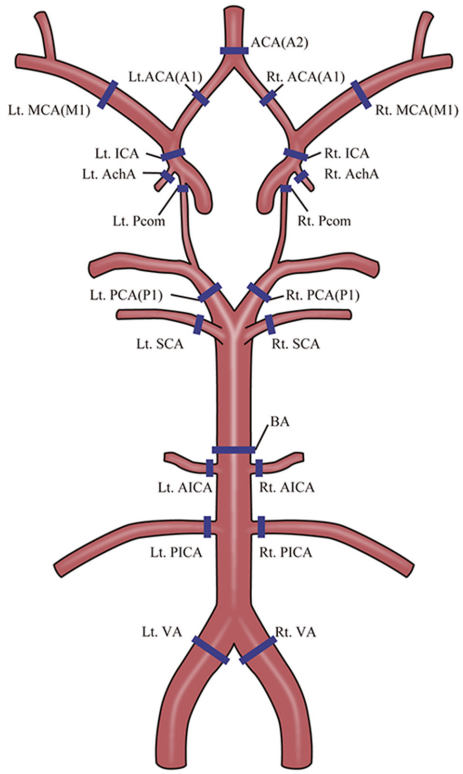

Fig. 2. Measured sites of cerebral artery diameter.

(BA) and the posterior communicating artery (P1). The BA was measured at the middle of the top of the BA and the union of bilateral vertebral arteries (BA trunk). The vertebral artery (VA) was measured proximal to the union of the BA. The posterior communicating artery (Pcom) and AchA were measured at the origin of the bifurcation from the ICA. The superior cerebellar artery (SCA) was measured at the origin of the bifurcation from the BA. The AICA and PICA were measured at the origin of the bifurcation from the BA or VA. The median and interquartile range (IQR) were calculated for each cerebral artery diameter. The Wilcoxon signed-rank test was used to determine whether there was a statistical difference in cerebral artery diameters between subjects. Moreover, the Holm's correction method was used to correct for multiplicity (Table 1, Supplementary Table 1). Pearson's correlation analysis was performed to assess whether weight and age had a relationship with the circumference of cerebral arteries (Table 2). Statistical analyses were performed using SPSS software version 26, and the level of statistical significance was set at $P<0.05$.

The Animal Care and Use Committee at Shiga University of Medical Science approved this study. In this experiment, 42 monkeys were euthanized per the regulations of our institution for experimental animals.

Table 1. The diameter of cerebral arteries of cynomolgus monkey in this study

	median	[IQR]	Group
BA trunk	1.37	[1.15, 1.52]	a
Lt.VA	1.14	[0.94, 1.30]	b
Rt.VA	1.03	[0.87, 1.22]	b
Lt.ICA	1.13	[1.02, 1.25]	b
Rt.ICA	1.10	[0.95, 1.29]	b
Lt.M1	0.87	[0.74, 1.00]	c
Rt.M1	0.91	[0.74, 1.00]	c
A2	0.68	[0.57, 0.77]	d
Lt.P1	0.68	[0.59, 0.78]	d
Rt.P1	0.69	[0.60, 0.82]	d
Lt.A1	0.61	[0.51, 0.76]	d,e
Rt.A1	0.62	[0.54, 0.73]	d,e,f
Lt.PICA	0.55	[0.45, 0.64]	f,g
Rt.PICA	0.54	[0.46, 0.61]	f,g
Lt.SCA	0.49	[0.46, 0.59]	g
Rt.SCA	0.49	[0.41, 0.53]	g
Lt.Pcom	0.47	[0.37, 0.62]	e,g,h
Rt.Pcom	0.46	[0.37, 0.54]	g,h
Lt.AchA	0.41	[0.32, 0.45]	h,i
Rt.AchA	0.40	[0.32, 0.43]	h,i
Lt.AICA	0.34	[0.26, 0.38]	i
Rt.AICA	0.33	[0.25, 0.39]	i

interquartile range (IQR) [25%, 75%]. There are significant differences between different groups, but there are no significant differences within the same group.

Results

Cerebrovascular structure

The ACA and MCA divide from the end of the ICA. The ACA divides medially and runs into the interhemispheric fissure. In 29 of 48 (60.4%) cases, the left and right ACAs merged (single type). In 16 (33.3%) cases, one ACA divided into two arteries near the confluence and then rejoined distally (fenestration type). In 3 (6.3%) cases, two ACAs (double ACA type) were found distally. In two of these three cases, the two arteries ran parallel to each other vertically. In the remaining one, two arteries merged distally (Fig. 3).

The MCA runs laterally after branching off the ICA. In total, 96 branching patterns of the horizontal section of this artery were analyzed. Bifurcation and trifurcation types were observed in 80 (83.3%) and 16 (16.7%) vessels, respectively.

The ICA branches into the Pcom and AchA, in that order, from the proximal side before branching into the ACA and MCA. The Pcom was lost in one case (2 vessels), and the AchA was lost in three cases (4 vessels) during brain sampling or artery stripping. The Pcom was confirmed in all 47 cases (94 vessels) examined. For the AchAs, 3 (3.3%) vessels were absent out of 45 cases (90 vessels).

In the posterior fossa, the bilateral VAs join to form the BA, and the bilateral PCA branch from the BA. The

Table 2. Correlation between cerebral artery diameter and weight and age

		Weight	Age
A2	Pearson's Correlation	0.050	0.188
	P-value	0.784	0.294
Lt.A1	Pearson's Correlation	0.292	−0.058
	P-value	0.099	0.750
Rt.A1	Pearson's Correlation	−0.111	0.055
	P-value	0.539	0.76
Lt.ICA	Pearson's Correlation	0.071	−0.042
	P-value	0.693	0.816
Rt.ICA	Pearson's Correlation	−0.135	0.100
	P-value	0.453	0.578
Lt.M1	Pearson's Correlation	0.068	0.276
	P-value	0.706	0.12
Rt.M1	Pearson's Correlation	−0.035	0.336
	P-value	0.846	0.056
Lt.AchA	Pearson's Correlation	0.037	−0.113
	P-value	0.840	0.533
Rt.AchA	Pearson's Correlation	0.034	0.092
	P-value	0.851	0.610
Lt.Pcom	Pearson's Correlation	−0.106	0.284
	P-value	0.555	0.109
Rt.Pcom	Pearson's Correlation	−0.165	0.169
	P-value	0.359	0.347
Lt.P1	Pearson's Correlation	0.064	0.024
	P-value	0.725	0.895
Rt.P1	Pearson's Correlation	0.072	0.122
	P-value	0.691	0.501
Lt.SCA	Pearson's Correlation	0.141	0.253
	P-value	0.435	0.155
Rt.SCA	Pearson's Correlation	0.087	0.174
	P-value	0.632	0.334
Lt.AICA	Pearson's Correlation	0.031	0.148
	P-value	0.865	0.411
Rt.AICA	Pearson's Correlation	0.026	−0.002
	P-value	0.885	0.991
Lt.PICA	Pearson's Correlation	0.197	−0.044
	P-value	0.271	0.810
Rt.PICA	Pearson's Correlation	0.048	0.177
	P-value	0.791	0.325
BA trunk	Pearson's Correlation	0.087	0.399*
	P-value	0.631	0.022
Lt.VA	Pearson's Correlation	0.232	0.217
	P-value	0.194	0.226
Rt.VA	Pearson's Correlation	0.113	0.389*
	P-value	0.531	0.025

*Correlation is significant at the $P<0.05$ level. Tests were two-tailed.

SCA bifurcates proximal to the PCA of the BA. The SCA could be identified in all cases. The branching pattern of the AICA and the PICA was examined at 96 sites on the left and right sides of 48 monkeys. A total of 66 (68.8%) sites, where both the AICA and PICA diverged from the BA and 9 (9.4%) sites, where the AICA diverged from the BA and PICA diverged from the VA, were observed. A total of 8 (8.3%) sites, where the AICA diverged from the BA and the two PICAs diverged from the BA and VA (double origin) were also observed. In cases of double origin, two vessels were fused distally. There were 2 (2.0%; one monkey) sites where both the AICA and PICA diverged from the VA. The common trunk of the AICA and PICA was found at 11 (11.5%) sites (Fig. 4).

Diameter of cerebral artery

The diameter of the BA was the largest and that of the ICA and VA was the second largest (Table 1). The AICA had the smallest diameter. The diameter of the cerebral artery gradually decreased peripherally (e.g., from the ICA to A1 and M1). However, the diameter of the distal ACA (A2) was larger than the horizontal section of the ACA (A1), although no significant difference was observed (Table 1).

We observed a weak positive correlation between age and most arteries, except Lt.A1, Lt.ICA, Lt.AchA, Rt.AICA, Lt.PICA, where a weak negative correlation was noted. However, a significant positive correlation between age and BA trunk as well as Rt.VA was observed. This clearly explains that age may not influence the diameter of each cerebral artery (Table 2).

There was a weak positive correlation between body weight and diameter of most arteries, except Rt.ICA, Rt.A1, Rt.M1, Lt.Pcom, and Rt.Pcom, where a weak negative correlation was noted. However, because there was no statistically significant correlation between any of the pairs analyzed, we concluded that the weight of the monkey does not influence cerebral arterial diameter (Table 2).

Discussion

In total, 93.7% of the cynomolgus monkeys studied here exhibited a single ACA, including the fenestration type. Although two distal ACAs were found in 6.3% of the cases, these arteries ran vertically-parallel, suggesting that these two arteries presumably corresponded to the pericallosal artery and the callosomarginal artery, rather than duplicated ACAs. Many primates, including cynomolgus monkeys have only a single distal ACA, also known as azygous ACA, which is however, only observed at a frequency of 0.2–4% in humans [16].

It is well-known that the ACA in humans exhibits several variations and anomalies depending on the degree of relative development of the left and right anterior cerebral artery and the median artery of the corpus callosum [17]. Azygous ACA is considered a remnant of

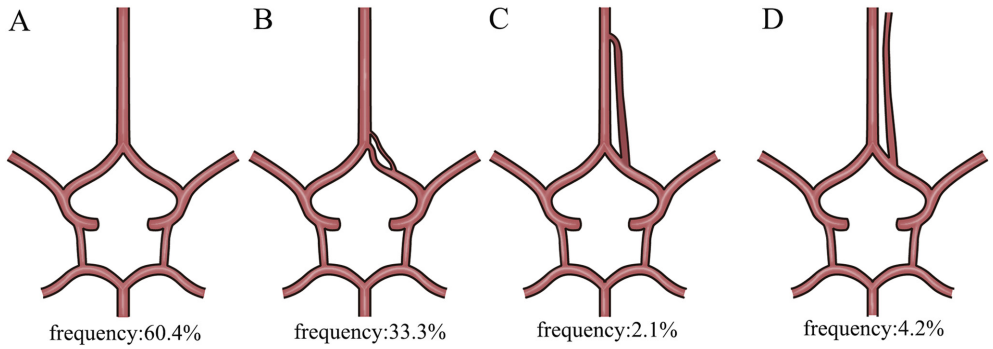

Fig. 3. The classification of the anterior cerebral artery (ACA) as single type (A), fenestration type (B), and double ACA type (C, D) based on macroscopic observations of its confluence.

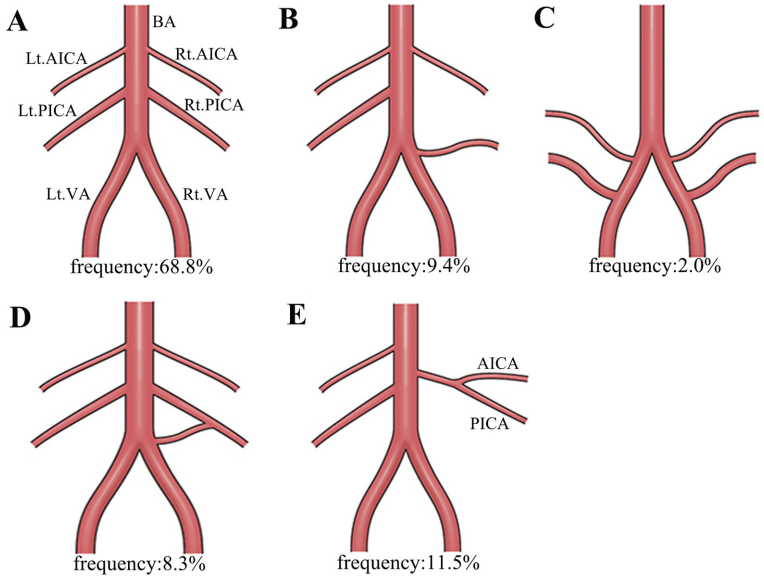

Fig. 4. Both the anterior inferior cerebellar artery (AICA) and the posterior inferior cerebellar artery (PICA) branch from the basilar artery (BA) (A). The AICA branches from the BA and the PICA branches from the vertebral artery (VA) (B). Both the AICA and the PICA branch from the VA (C). The VA branches from the BA. The PICA is double origin type that one branch comes from the VA, while the other branch originates from the BA, which merge into one distally (D). The common trunk of the AICA and the PICA branch from the BA (E).

the median artery of the corpus callosum in humans [18, 19]. The single artery at the distal part of ACA in cynomolgus monkeys is likely to develop in a similar manner.

The frequency of ACA fenestration in cynomolgus monkeys is reported to be 33.3%, which is higher than the observed range of between 0.1% and 4.9% in humans [20]. The ACA fenestration in humans often occurs distal to the horizontal part of the anterior ACA [21, 22]. The primary olfactory arteries on both sides form a plexiform anastomosis at the distal end during developmental, and the remnant of anastomosis forms fenestration of the ACA [18]. Although it is previously reported that 46% of ACAs include an anterior communicating artery in rhesus monkeys, which belong to the same family as cynomolgus monkeys [2], it seems to be a fenestration rather than the anterior communicating artery. Since fenestration was more frequently observed in cynomolgus monkeys, the development of vasculogenesis in this species could thus be less compared to that in humans.

Regarding the branching patterns of the MCA in cynomolgus monkeys, the bifurcation type was the most common, followed by the trifurcation type. Studies have reported that the frequency of monofurcation-, bifurcation-, trifurcation-, and the tetrafurcation-types to be in the ranges of 3.8–17.0%, 64.3–92.7%, 7.3–28.6%, and 0.7–3.8%, respectively, in humans [13, 23–27]. In both cynomolgus monkeys and humans, the bifurcation type was the most common, followed by the trifurcation type.

In humans, the AchA is rarely absent [28], and the P.com is absent in the range of about: 1–10% [29–31]; however, regression or the lack of the P.com was not observed in cynomolgus monkeys.

Few reports exist regarding the cerebellar arteries of primates. Only one report on the cerebellar artery of baboons showed a common trunk of the AICA and PICA [4]. The basic structure of the human cerebellar artery is that the PICA branches from the distal side of the vertebral artery, the AICA branches from the proximal-middle part of the BA, and the SCA branches from the proximal side of the BAs terminal. However, studies reported that these arteries in humans highly varies, as they are formed from the transverse artery branching from the longitudinal neural arteries during the fetal period according to blood flow demands from the cerebellum and brainstem [32]. No defects were observed in the SCA in humans [33]. The frequency of absence of PICA in one side is in the range of 15–26%, while the absence in both sides is in the range of 2–2.5% [34]. The AICA is absent in one side in 3.1–18.5% [35, 36]. In the absence of either the AICA or the PICA, blood flow can be supplied from the other artery when a complementary relationship is present [37]. The common trunk of the AICA and PICA is frequently present (22.1%) [36]. The PICA may instead diverge from the basilar trunk [38], and the AICA may diverge from the vertebrobasilar junction or the VA [36], however, at a very low frequency. The frequency occurrence of double origin of the PICA is in the range of 1.45–6% [39, 40], and the double origin of the AICA occurs at 10.4% [36]. In this study, The SCA was present in all cases, and the inferior cerebellar arteries had the most common pattern in which both the AICA and PICA diverged from the BAs in cynomolgus monkey. The common trunk of the AICA and PICA was found in 11.5%, and the double origin of the PICA was found in 8.3%. As in humans, cynomolgus monkeys have many variations in the cerebellar arteries, however the difference from humans is that both AICA and PICA often branch from the BAs.

The diameter of ICA is larger than that of BA in human cerebral arteries [41, 42], however, the opposite is true for cynomolgus monkey. In human azygous ACA, the diameter of the distal ACA was larger than the horizontal part of the ACA (A1) [43], and the results were similar in cynomolgus monkeys. The diameter of the P.com in humans greatly varies due to developmental variations, such as the fetal type and adult type of posterior cerebral circulation [44]. In the case of fetal type of posterior cerebral circulation, the PCA is supplied by the P.com; however in adult type, the PCA is supplied by the BA. Therefore, the diameter of the P.com in the fetal type is larger than that in the adult type. The diameter of the P.com in cynomolgus monkeys also varied widely, presumably due to the presence of two types of posterior cerebral circulation in humans.

In the present study, the diameter of the cerebral artery of cynomolgus monkeys was not significantly correlated with age and body weight. It has been reported that the diameter of the ICA and ACA in human adults is significantly correlated with age [45, 46]. In adult human, the increase in cerebral artery diameter with increasing age is believed to be due to vascular remodeling by arteriosclerosis [47, 48]. We could not find any study directly investigating the relationship between body weight and cerebral artery diameter. However, as it is known that obesity promotes arteriosclerosis [49–51], it is possible that obesity affects the diameter of the cerebral artery. Arteriosclerosis is absent in other mammals and is believed to be a pathological condition peculiar to humans [52]. The fact that arteriosclerosis is absent in cynomolgus monkeys could explain the lack of difference in the cerebral artery diameter depending on age and body weight.

Few detailed studies evaluating the diameter and structure of the cerebral artery in cynomolgus monkeys are available. In the monkey cerebral infarction model, the MCA is occluded with a balloon catheter or an autologous clot to induce cerebral infarction [53]. Thus, clarifying the normal diameter of the cerebral artery could help determine the material and size of the embolic substance. In the monkey cerebral aneurysm model, the unilateral carotid artery is ligated to increase hemodynamic stress on the contralateral carotid artery [54]. Further information about the normal diameter may thus be useful for assessing changes in the diameter due to hemodynamic stress.

One limitation of this study is that the monkeys used were female, since females are predominantly used for medical experiments at the study institution. Male monkeys are kept in small numbers for breeding purposes only. Some reports have found that the cerebrovascular diameter in males was significantly larger than in females [45, 55]. Therefore, as in humans, monkeys may have larger cerebrovascular diameters in males than in females.

Conclusion

In cynomolgus monkey, the vascular structure was similar to that of humans, except for only a single distal ACA, and the origin of the inferior cerebellar arteries was mostly the basilar trunk. Although the ICA was larger than the BAs in humans, the BAs exhibited the

largest diameter in cynomolgus monkeys. We expect that this anatomical information will aid in furthering the research on cerebrovascular disease using cynomolgus monkeys.

Conflict of Interest

The authors declare that they have no conflicts of interest.

Acknowledgments

This work was supported by JSPS KAKENHI Grant Number JP19K09524. We would like to thank Mr. Ikuo Kawamoto and Mr. Mitsuru Murase (Animal care and research support specialists belonging to Research Center for Animal Life Science at Shiga University of Medical Science) for helping us sedation during euthanasia of monkeys.

References

1. Watts JW. A comparative study of the anterior cerebral artery and the circle of Willis in primates. J Anat. 1934; 68: 534–550. [Medline]
2. Kassel NF, Langfitt TW. Variations in the circle of Willis in Macaca mulatta. Anat Rec. 1965; 152: 257–263. [Medline] [CrossRef]
3. Kapoor K, Kak VK, Singh B. Morphology and comparative anatomy of circulus arteriosus cerebri in mammals. Anat Histol Embryol. 2003; 32: 347–355. [Medline] [CrossRef]
4. Lake AR, Van Niekerk IJ, Le Roux CG, Trevor-Jones TR, De Wet PD. Angiology of the brain of the baboon Papio ursinus, the vervet monkey Cercopithecus pygerithrus, and the bush-baby Galago senegalensis. Am J Anat. 1990; 187: 277–286. [Medline] [CrossRef]
5. Nikzad S, Tan SG, Yong Seok Yien C, Ng J, Alitheen NB, Khan R, et al. Genetic diversity and population structure of long-tailed macaque (Macaca fascicularis) populations in Peninsular Malaysia. J Med Primatol. 2014; 43: 433–444. [Medline] [CrossRef]
6. Espinosa F, Weir B, Overton T, Castor W, Grace M, Boisvert D. A randomized placebo-controlled double-blind trial of nimodipine after SAH in monkeys. Part 1: Clinical and radiological findings. J Neurosurg. 1984; 60: 1167–1175. [Medline] [CrossRef]
7. Findlay JM, Weir BK, Steinke D, Tanabe T, Gordon P, Grace M. Effect of intrathecal thrombolytic therapy on subarachnoid clot and chronic vasospasm in a primate model of SAH. J Neurosurg. 1988; 69: 723–735. [Medline] [CrossRef]
8. Macdonald RL, Weir BK, Runzer TD, Grace MG, Findlay JM, Saito K, et al. Etiology of cerebral vasospasm in primates. J Neurosurg. 1991; 75: 415–424. [Medline] [CrossRef]
9. Pluta RM, Deka-Starosta A, Zauner A, Morgan JK, Muraszko KM, Oldfield EH. Neuropeptide Y in the primate model of subarachnoid hemorrhage. J Neurosurg. 1992; 77: 417–423. [Medline] [CrossRef]
10. Kito G, Nishimura A, Susumu T, Nagata R, Kuge Y, Yokota C, et al. Experimental thromboembolic stroke in cynomolgus monkey. J Neurosci Methods. 2001; 105: 45–53. [Medline] [CrossRef]
11. D'Arceuil HE, Duggan M, He J, Pryor J, de Crespigny A. Middle cerebral artery occlusion in Macaca fascicularis: acute and chronic stroke evolution. J Med Primatol. 2006; 35: 78–86. [Medline] [CrossRef]
12. Schneider CA, Rasband WS, Eliceiri KW. NIH Image to ImageJ: 25 years of image analysis. Nat Methods. 2012; 9: 671–675. [Medline] [CrossRef]
13. Umansky F, Juarez SM, Dujovny M, Ausman JI, Diaz FG, Gomes F, et al. Microsurgical anatomy of the proximal segments of the middle cerebral artery. J Neurosurg. 1984; 61: 458–467. [Medline] [CrossRef]
14. Tao X, Yu XJ, Bhattarai B, Li TH, Jin H, Wei GW, et al. Microsurgical anatomy of the anterior communicating artery complex in adult Chinese heads. Surg Neurol. 2006; 65: 155–161, discussion 161. [Medline] [CrossRef]
15. Kedia S, Daisy S, Mukherjee KK, Salunke P, Srinivasa R, Narain MS. Microsurgical anatomy of the anterior cerebral artery in Indian cadavers. Neurol India. 2013; 61: 117–121. [Medline] [CrossRef]
16. Lehecka M, Porras M, Dashti R, Niemelä M, Hernesniemi JA. Anatomic features of distal anterior cerebral artery aneurysms: a detailed angiographic analysis of 101 patients. Neurosurgery. 2008; 63: 219–228, discussion 228–229. [Medline] [CrossRef]
17. Baptista AG. Studies on the arteries of the brain. The anterior cerebral artery: some anatomic features and their clinical implications. Neurology. 1963; 13: 825–835. [Medline] [CrossRef]
18. Okahara M, Kiyosue H, Mori H, Tanoue S, Sainou M, Nagatomi H. Anatomic variations of the cerebral arteries and their embryology: a pictorial review. Eur Radiol. 2002; 12: 2548–2561. [Medline] [CrossRef]
19. Parmar H, Sitoh YY, Hui F. Normal variants of the intracranial circulation demonstrated by MR angiography at 3T. Eur J Radiol. 2005; 56: 220–228. [Medline] [CrossRef]
20. Cilliers K, Page BJ. Review of the anatomy of the distal anterior cerebral artery and its anomalies. Turk Neurosurg. 2016; 26: 653–661. [Medline]
21. Choudhari KA. Fenestrated anterior cerebral artery. Br J Neurosurg. 2002; 16: 525–529. [Medline] [CrossRef]
22. Uchino A, Nomiyama K, Takase Y, Kudo S. Anterior cerebral artery variations detected by MR angiography. Neuroradiology. 2006; 48: 647–652. [Medline] [CrossRef]
23. Gibo H, Carver CC, Rhoton AL Jr, Lenkey C, Mitchell RJ. Microsurgical anatomy of the middle cerebral artery. J Neurosurg. 1981; 54: 151–169. [Medline] [CrossRef]
24. Umansky F, Dujovny M, Ausman JI, Diaz FG, Mirchandani HG. Anomalies and variations of the middle cerebral artery: a microanatomical study. Neurosurgery. 1988; 22: 1023–1027. [Medline] [CrossRef]
25. Vuillier F, Medeiros E, Moulin T, Cattin F, Bonneville JF, Tatu L. Main anatomical features of the M1 segment of the middle cerebral artery: a 3D time-of-flight magnetic resonance angiography at 3 T study. Surg Radiol Anat. 2008; 30: 509–514. [Medline] [CrossRef]
26. Ogeng'o JA, Njongo W, Hemed E, Obimbo MM, Gimongo J. Branching pattern of middle cerebral artery in an African population. Clin Anat. 2011; 24: 692–698. [Medline] [CrossRef]
27. Sadatomo T, Yuki K, Migita K, Imada Y, Kuwabara M, Kurisu K. Differences between middle cerebral artery bifurcations with normal anatomy and those with aneurysms. Neurosurg Rev. 2013; 36: 437–445. [Medline] [CrossRef]
28. Carpenter MB, Noback CR, Moss ML. The anterior choroidal artery; its origins course, distribution, and variations. AMA Arch Neurol Psychiatry. 1954; 71: 714–722. [Medline] [CrossRef]
29. Eftekhar B, Dadmehr M, Ansari S, Ghodsi M, Nazparvar B, Ketabchi E. Are the distributions of variations of circle of Willis different in different populations? - Results of an anatomical study and review of literature. BMC Neurol. 2006; 6: 22.

[Medline] [CrossRef]
30. Kapoor K, Singh B, Dewan LI. Variations in the configuration of the circle of Willis. Anat Sci Int. 2008; 83: 96–106. [Medline] [CrossRef]
31. Gunnal SA, Farooqui MS, Wabale RN. Anatomical variability of the posterior communicating artery. Asian J Neurosurg. 2018; 13: 363–369. [Medline] [CrossRef]
32. Chen MM, Chen SR, Diaz-Marchan P, Schomer D, Kumar VA. Anterior inferior cerebellar artery strokes based on variant vascular anatomy of the posterior circulation: clinical deficits and imaging territories. J Stroke Cerebrovasc Dis. 2018; 27: e59–e64. [Medline] [CrossRef]
33. Pekcevik Y, Pekcevik R. Variations of the cerebellar arteries at CT angiography. Surg Radiol Anat. 2014; 36: 455–461. [Medline] [CrossRef]
34. Macchi V, Porzionato A, Parenti A, De Caro R. The course of the posterior inferior cerebellar artery may be related to its level of origin. Surg Radiol Anat. 2004; 26: 60–65. [Medline] [CrossRef]
35. Akgun V, Battal B, Bozkurt Y, Oz O, Hamcan S, Sari S, et al. Normal anatomical features and variations of the vertebrobasilar circulation and its branches: an analysis with 64-detector row CT and 3T MR angiographies. ScientificWorldJournal. 2013; 2013: 620162. [Medline] [CrossRef]
36. Hou K, Li G, Luan T, Xu K, Xu B, Yu J. Anatomical study of anterior inferior cerebellar artery and its reciprocal relationship with posterior inferior cerebellar artery based on angiographic data. World Neurosurg. 2020; 133: e459–e472. [Medline] [CrossRef]
37. Lister JR, Rhoton AL Jr, Matsushima T, Peace DA. Microsurgical anatomy of the posterior inferior cerebellar artery. Neurosurgery. 1982; 10: 170–199. [Medline] [CrossRef]
38. Macchi V, Porzionato A, Guidolin D, Parenti A, De Caro R. Morphogenesis of the posterior inferior cerebellar artery with three-dimensional reconstruction of the late embryonic vertebrobasilar system. Surg Radiol Anat. 2005; 27: 56–60. [Medline] [CrossRef]
39. Fujii K, Lenkey C, Rhoton AL Jr. Microsurgical anatomy of the choroidal arteries. Fourth ventricle and cerebellopontine angles. J Neurosurg. 1980; 52: 504–524. [Medline] [CrossRef]
40. Lesley WS, Rajab MH, Case RS. Double origin of the posterior inferior cerebellar artery: association with intracranial aneurysm on catheter angiography. AJR Am J Roentgenol. 2007; 189: 893–897. [Medline] [CrossRef]
41. Krabbe-Hartkamp MJ, van der Grond J, de Leeuw FE, de Groot JC, Algra A, Hillen B, et al. Circle of Willis: morphologic variation on three-dimensional time-of-flight MR angiograms. Radiology. 1998; 207: 103–111. [Medline] [CrossRef]
42. Moore S, David T, Chase JG, Arnold J, Fink J. 3D models of blood flow in the cerebral vasculature. J Biomech. 2006; 39: 1454–1463. [Medline] [CrossRef]
43. Wan-Yin S, Ming-Hua L, Bin-Xian G, Yong-Dong L, Hua-Qiao T. Azygous anterior cerebral artery and associated aneurysms: detection and identification using 3-dimensional time-of-flight magnetic resonance angiography. J Neuroimaging. 2014; 24: 18–22. [Medline] [CrossRef]
44. Pai BS, Varma RG, Kulkarni RN, Nirmala S, Manjunath LC, Rakshith S. Microsurgical anatomy of the posterior circulation. Neurol India. 2007; 55: 31–41. [Medline] [CrossRef]
45. Cilliers K, Page BJ. Description of the anterior cerebral artery and its cortical branches: Variation in presence, origin, and size. Clin Neurol Neurosurg. 2017; 152: 78–83. [Medline] [CrossRef]
46. Cogswell PM, Lants SK, Davis LT, Donahue MJ. Vessel wall and lumen characteristics with age in healthy participants using 3T intracranial vessel wall magnetic resonance imaging. J Magn Reson Imaging. 2019; 50: 1452–1460. [Medline] [CrossRef]
47. Qiao Y, Anwar Z, Intrapiromkul J, Liu L, Zeiler SR, Leigh R, et al. Patterns and implications of intracranial arterial remodeling in stroke patients. Stroke. 2016; 47: 434–440. [Medline] [CrossRef]
48. Zhu XJ, Du B, Lou X, Hui FK, Ma L, Zheng BW, et al. Morphologic characteristics of atherosclerotic middle cerebral arteries on 3T high-resolution MRI. AJNR Am J Neuroradiol. 2013; 34: 1717–1722. [Medline] [CrossRef]
49. Beltowski J. Leptin and atherosclerosis. Atherosclerosis. 2006; 189: 47–60. [Medline] [CrossRef]
50. Fantuzzi G, Mazzone T. Adipose tissue and atherosclerosis: exploring the connection. Arterioscler Thromb Vasc Biol. 2007; 27: 996–1003. [Medline] [CrossRef]
51. Ruscica M, Baragetti A, Catapano AL, Norata GD. Translating the biology of adipokines in atherosclerosis and cardiovascular diseases: Gaps and open questions. Nutr Metab Cardiovasc Dis. 2017; 27: 379–395. [Medline] [CrossRef]
52. Kawanishi K, Dhar C, Do R, Varki N, Gordts PLSM, Varki A. Human species-specific loss of CMP-*N*-acetylneuraminic acid hydroxylase enhances atherosclerosis via intrinsic and extrinsic mechanisms. Proc Natl Acad Sci USA. 2019; 116: 16036–16045. [Medline] [CrossRef]
53. Wu D, Chen J, Wang B, Zhang M, Shi J, Ma Y, et al. Endovascular ischemic stroke models of adult rhesus monkeys: a comparison of two endovascular methods. Sci Rep. 2016; 6: 31608. [Medline] [CrossRef]
54. Hashimoto N, Kim C, Kikuchi H, Kojima M, Kang Y, Hazama F. Experimental induction of cerebral aneurysms in monkeys. J Neurosurg. 1987; 67: 903–905. [Medline] [CrossRef]
55. Müller HR, Brunhölzl C, Radü EW, Buser M. Sex and side differences of cerebral arterial caliber. Neuroradiology. 1991; 33: 212–216. [Medline] [CrossRef]